nature cities

Supplementary information

https://doi.org/10.1038/s44284-025-00300-3

Environmental burden and health inequity in China's road-based express delivery

In the format provided by the authors and unedited

CONTENTS

This Supplementary Information document contains 26 pages organized as follows:

Section S1 Uncertainty of GHG and Air Pollutant Emission for Express Delivery

We conducted a comprehensive uncertainty analysis for emission estimation using Monte Carlo simulation. Three key parameters that contribute most significantly to emission uncertainties: parcel weight, rated truck payload capacity, and truck loading ratio. Specifically, the parcel weight was determined to be 1.6 ± 0.9 kg with a coefficient of variation (CV) of 54%[1-3]. For vehicle parameters, the rated payload capacity of heavy-duty trucks used in inter-city logistics was 10.5 ± 1.5 t (CV=14.7%), derived from surveying 69 inter-city delivery trucks on https://www.autohome.com.cn/. While light-duty trucks for intra-city delivery had an average rated payload capacity of 2.0 ± 0.7 t (CV=32.2%), based on a survey of 34 common urban delivery vehicles. The truck loading ratio was assigned a CV of 20% based on empirical data. We performed 10,000 Monte Carlo simulations to assess the combined effect of these uncertainties, with the 25th and 75th percentiles of the simulation results defining the uncertainty range of our emission estimates.

Section S2 Multi-Resolution Validation of Cross-Regional Pollution Patterns

To validate the applicability of our cross-regional analysis conclusions at different resolutions, we complemented our GEOS-Chem modeling with high-resolution WRF-Chem simulations (9 km) for representative months (January, April, July, and October 2021) over eastern China, encompassing major urban agglomerations and transit corridors. The finding that major transit regions bear disproportionate pollution burdens was robust across both modeling resolutions.

The models showed strong agreement for both baseline concentrations and express delivery contributions, with both consistently showing higher pollutant levels in transit regions (Table S4). Using NO_2 as a representative pollutant due to its transportation relevance[4] and relatively short lifetime[5], our comparison of express delivery contributions confirmed similar spatial distributions between the two models (Fig. S8). The high-resolution WRF-Chem simulations revealed additional detail, showing that highways and their surrounding areas (10-km buffer zones) experienced the highest express delivery NO_2 contributions, averaging 0.25 $\mu g \cdot m^{-3}$, 1.5 times higher than the simulation domain average. This concentration gradient along transportation corridors demonstrates the spatial correlation between express delivery networks and pollution patterns at finer resolution. The highest urban NO_2 contributions from express delivery were found in Jinhua and Guangzhou (China's first and second-ranked express delivery cities), reaching 1.27 and 1.13 $\mu g \cdot m^{-3}$, respectively.

Section S3 GHG Emissions from Air Transport in Express Delivery

We estimated GHG emissions from air transport in express delivery (E_{AF}) using the following formula:

$$E_{AF} = \sum_i^n Distance_i \times P_i \times EF \times W \quad (1)$$

Where *EF* represents the aviation GHG emission factor per unit transport volume, calculated based on the official guidance document[6] and SF Express Holdings' 2019 Sustainability Report. $Distance_i$ is the transport distance for each air route *i*, calculated using great-circle distances between airports, and P_i is the number of parcels on each route. *w* is the average weight of air-transported parcels. In the absence of comprehensive weight distribution data for air-transported parcels, we applied a conservative approach by estimating their average weight at 50% of road-transported parcels, reflecting industry practices where air transport predominantly handles lower-mass shipments.

This methodology yielded total GHG emissions from air transport in China's express delivery sector of 3.02 Mt CO_2e in 2021, with a mean air route distance of 1,017 km. The approach may introduce considerable uncertainties. Our collected waybill data contain only airport-to-airport information without detailed flight paths, while actual flight trajectories frequently deviate from great-circle paths due to air traffic management protocols, potentially introducing systematic errors in spatial emission allocation[7]. Additionally, the paucity of reliable weight data for air-transported parcels necessitates parameter assumptions that could affect emission calculations. Given the high emission uncertainties, we excluded air freight transport emissions from our main cross-regional analysis.

Section S4 Waybill Data Processing and Flow Pattern Validation

We collected 824,508 express delivery waybills from 2021, extracting detailed routing information after data anonymization. Each waybill record contains origin and destination locations, intermediate collection or distribution centers (Table S1). To address potential bias from single-company data while maintaining consistent city-to-city delivery proportions, we implemented random sampling of waybills for each city to align with official municipal delivery volume proportions. The final dataset comprises 688,415 waybills, including 598,983 inter-city deliveries.

Given the limited availability of national-scale express delivery flow data in China, we validated our data using intra-regional parcel flow patterns. Specifically, we compared the proportion of parcels flowing from the top two cities to other cities within their respective regions: Beijing and Tianjin in BTH, Guangzhou and Shenzhen in PRD, Suzhou and Nantong in Jiangsu, and Jinhua

and Hangzhou in Zhejiang. The validation was conducted against data from Kuaidi100 (China's leading express delivery tracking platform, https://zhuanlan.zhihu.com/p/450238728), which was derived from their analysis of 12.97 million deliveries (1.67 million for BTH, 7.04 million for YRD, 1.80 million for Jiangsu, and 2.46 million for Zhejiang). Our flow proportions showed strong correlation with Kuaidi100's data (R^2=0.9, Fig. S12).

The inter-city waybills were decomposed into origin-transit, transit-transit, and transit-destination segments, generating 1.012 million city-to-city transportation records. While 5.9% of inter-city parcels involve air transportation, only their road transportation segments were included in this analysis.

Section S5 GEOS-Chem Model Performance

The GEOS-Chem simulation was validated using observational data from China Ministry of Ecology and Environment (MEE) surface measurement network. Model performance evaluation showed strong agreement between simulated and observed $PM_{2.5}$ concentrations at daily scale across China (R=0.86, NMB=-13.2%). The model effectively captured $PM_{2.5}$ patterns in major urban agglomerations (BTH: R=0.67, NMB=-4.0%; YRD: R=0.80, NMB=6.4%; PRD: R=0.71, NMB=-6.8%) (Fig. S15). Comparison between observed and GEOS-Chem simulated daily NO_2 concentrations showed similarly strong performance across China (R=0.87, NMB=-13.6%) and in three major urban agglomerations (BTH: R=0.76, NMB=-13.8%; YRD: R=0.76, NMB=12.7%; PRD: R=0.63, NMB=11.8%) (Fig. S16). Annual mean simulated concentrations ($PM_{2.5}$: 27.9 $\mu g \cdot m^{-3}$; NO_2: 22.0 $\mu g \cdot m^{-3}$) also aligned well with observations ($PM_{2.5}$: 32.1 $\mu g \cdot m^{-3}$; NO_2: 25.5 $\mu g \cdot m^{-3}$).

Incorporating express delivery emissions improved model performance, particularly in regions with high delivery activities. We identified 541 monitoring stations in or within 5 arcmin distance of high-emission grids (defined as grids with express delivery emissions exceeding 25 t per 5 arcmin) (Fig. S17). The improvement was pronounced at stations near high-emission areas, where the bias in $PM_{2.5}$ decreased by 99.7 $ng \cdot m^{-3}$ and in NO_2 by 298.5 $ng \cdot m^{-3}$. Similarly, the normalized mean bias (NMB) of $PM_{2.5}$ and NO_2 showed improvement in high-emission areas (0.30% and 0.80% reduction), demonstrating the model's enhanced capability in capturing the spatial heterogeneity of express delivery-related pollution.

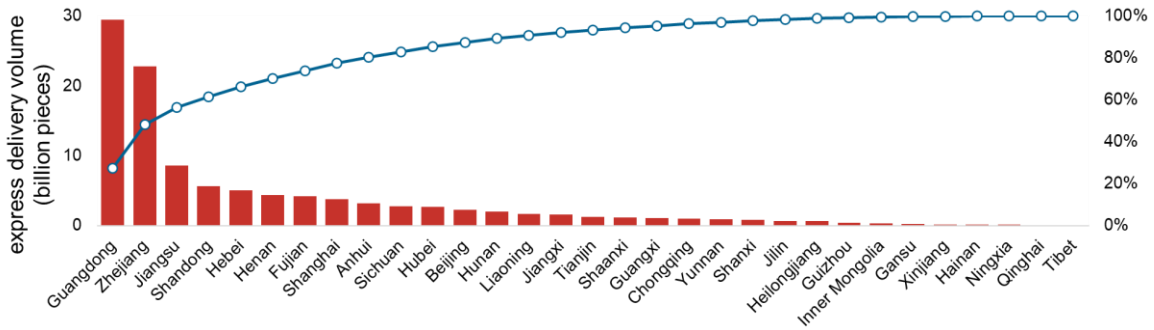

Fig. S1 | Express delivery volume in each province in 2021.

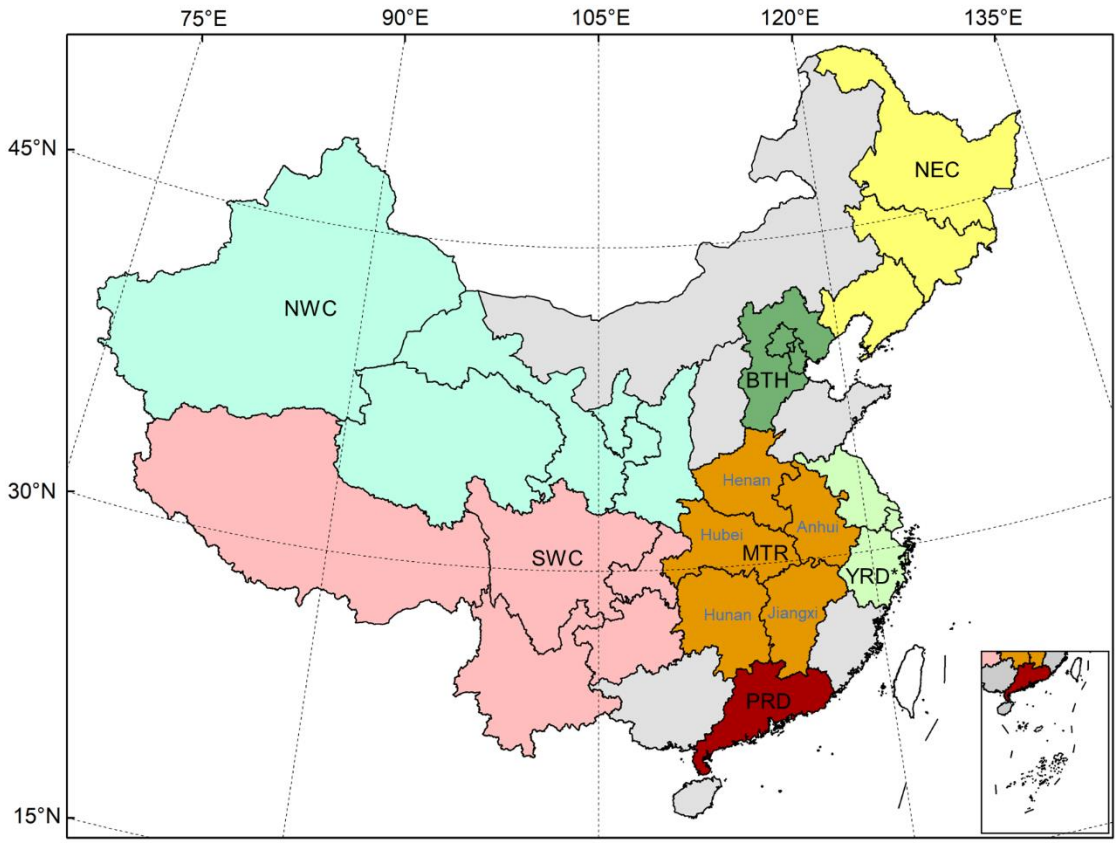

Fig. S2 | Geospatial boundaries of major regions in China. BTH (Beijing-Tianjin-Hebei), YRD* (Yangtze River Delta excluding Anhui province), PRD (Pearl River Delta), MTR (major transit regions), NEC (Northeast China), NWC (Northwest China) and SWC (Southwest China) are shown in different colors. Henan, Hubei and Hunan provinces constitute Central China, which is part of the major transit regions (MTR). The map was created using ArcGIS (v10.8, Esri), with administrative boundaries from the Standard Map Service System, Ministry of Natural Resources of China (http://bzdt.ch.mnr.gov.cn/index.html).

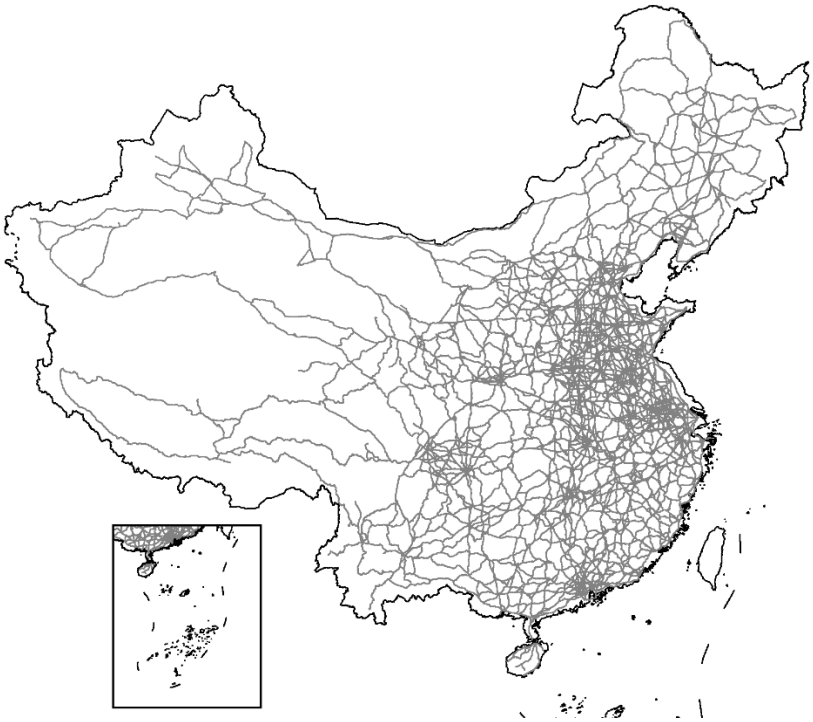

Fig.S3 | Route identification of inter-city express delivery in China. The map was created using ArcGIS (v10.8, Esri), with administrative boundaries from the Standard Map Service System, Ministry of Natural Resources of China (http://bzdt.ch.mnr.gov.cn/index.html).

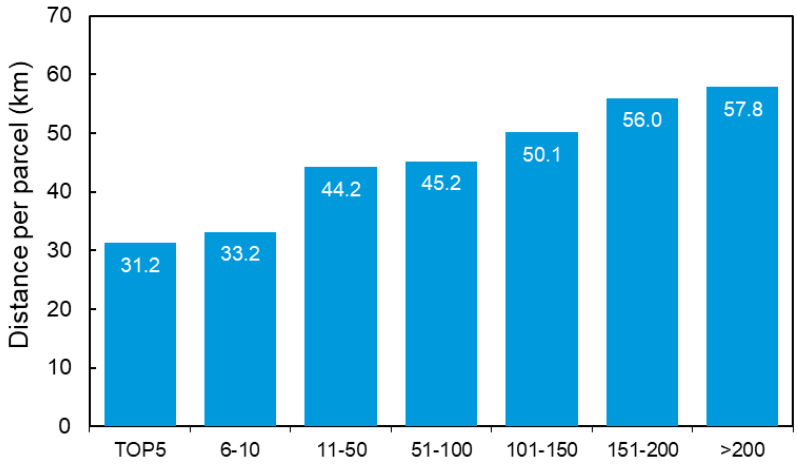

Fig. S4 | Average intra-city delivery distances across different city tiers based on intra-city delivery volume rankings (top 5, 6-10, 11-50, 51-100, 101-150, 151-200, and >200).

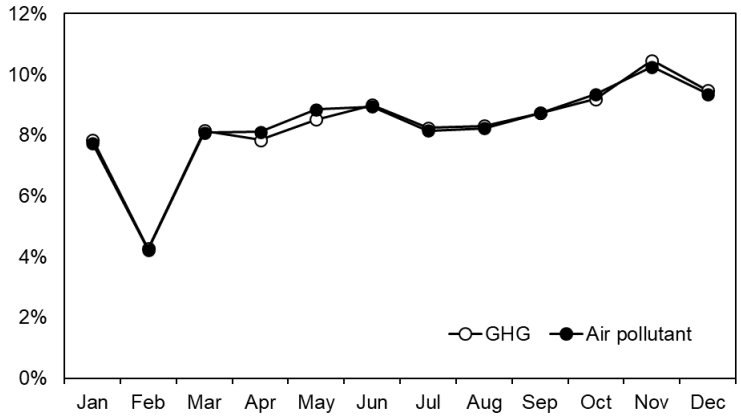

Fig. S5 | Temporal variations in GHG and air pollutant emissions from express delivery transportation.

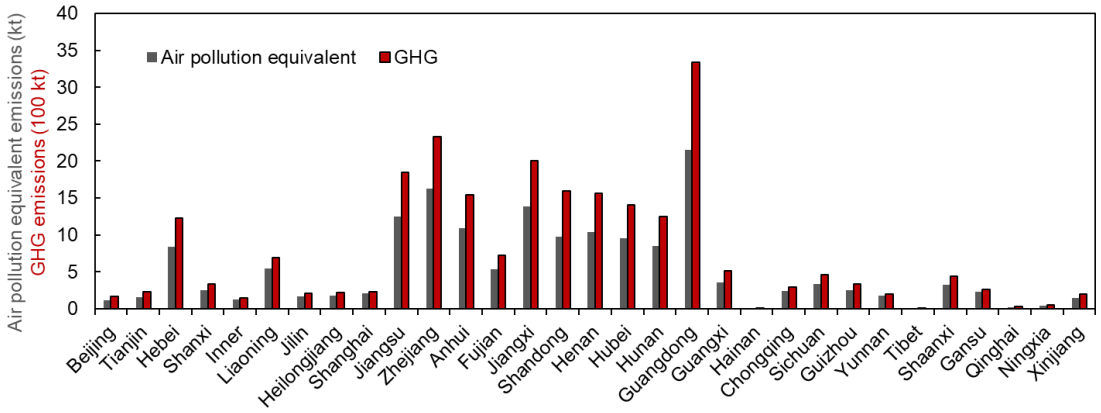

Fig. S6 | Provincial distribution of GHG and air pollutant emissions from express delivery transportation.

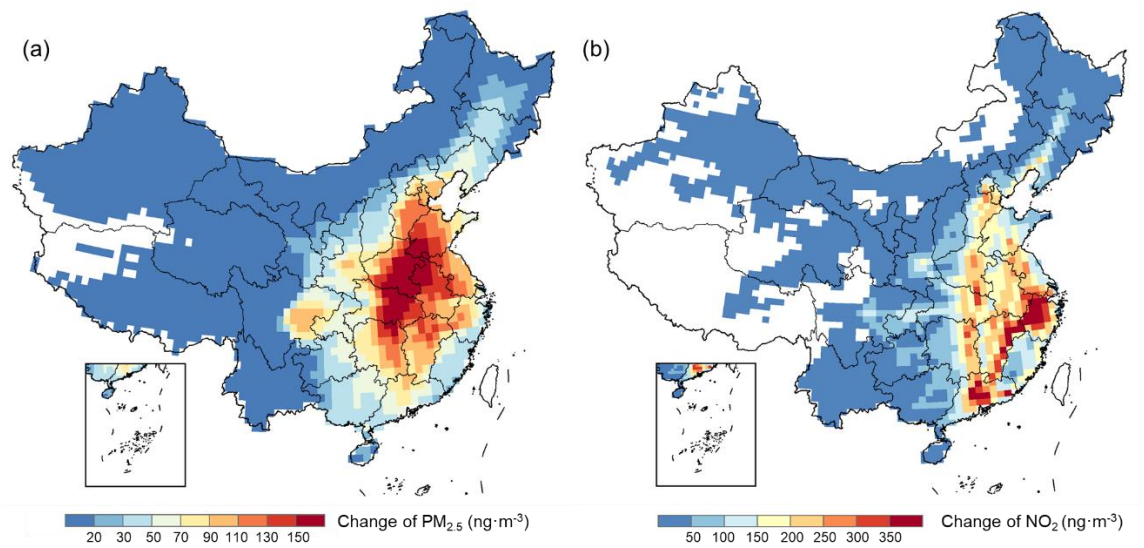

Fig. S7 | Contribution of express delivery transportation to annual averaged $PM_{2.5}$ and NO_2 concentrations. Changes in $PM_{2.5}$ (a) and NO_2 (b) concentrations were quantified by comparing GEOS-Chem simulations with and without express delivery emissions. Maps were created using ArcGIS (v10.8, Esri), with administrative boundaries from the Standard Map Service System, Ministry of Natural Resources of China (http://bzdt.ch.mnr.gov.cn/index.html).

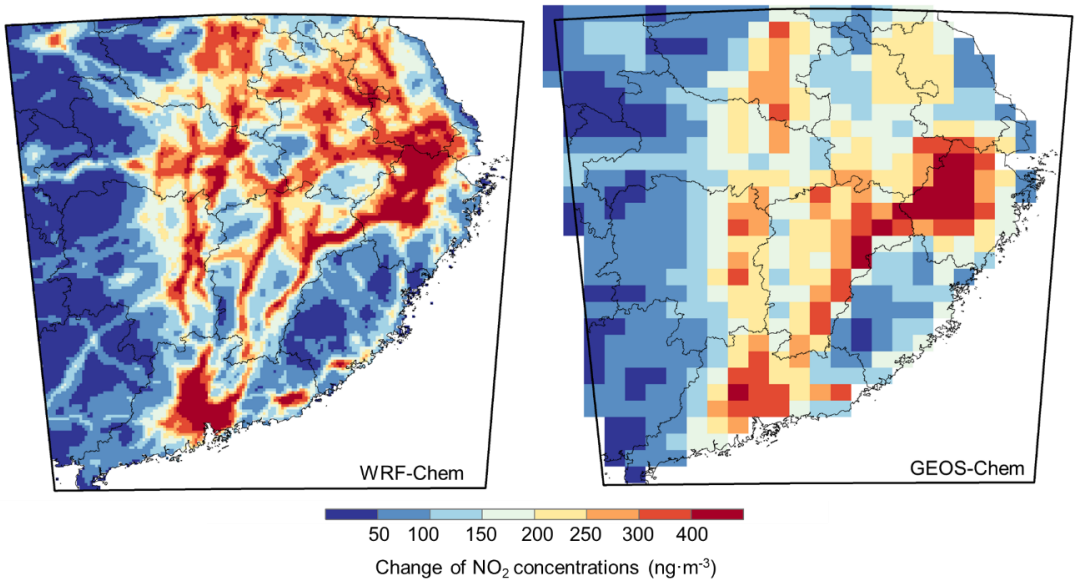

Fig. S8 | Spatial distribution of express delivery contribution to NO_2 concentrations ($ng \cdot m^{-3}$) from high-resolution WRF-Chem simulations (9 km) and GEOS-Chem simulations (0.5° × 0.625°), averaged for January, April, July, and October 2021. Both models exhibit similar spatial distributions, showing strong correlation with major express transportation corridors and highlighting the influence of transportation networks on regional pollution patterns. Maps were created using ArcGIS (v10.8, Esri), with administrative boundaries from the Standard Map Service System, Ministry of Natural Resources of China (http://bzdt.ch.mnr.gov.cn/index.html).

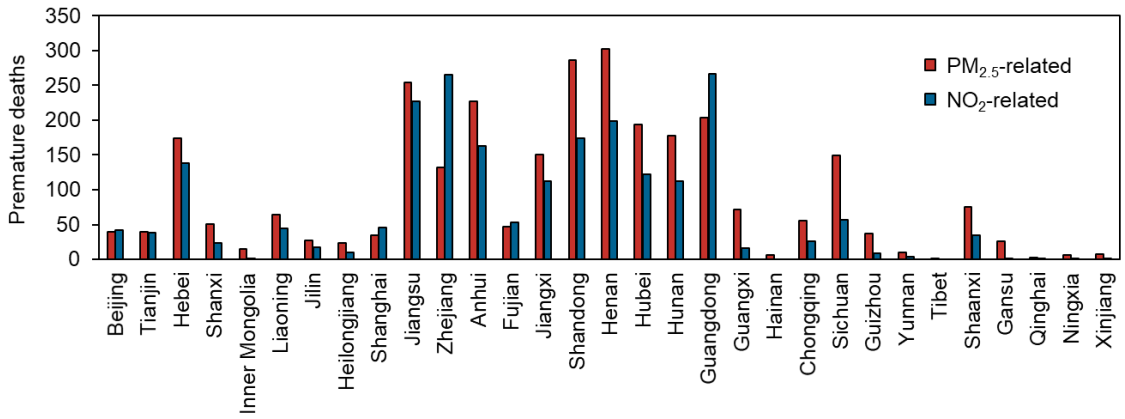

Fig. S9 | Provincial $PM_{2.5}$- and NO_2- related premature deaths attributable to express delivery emissions.

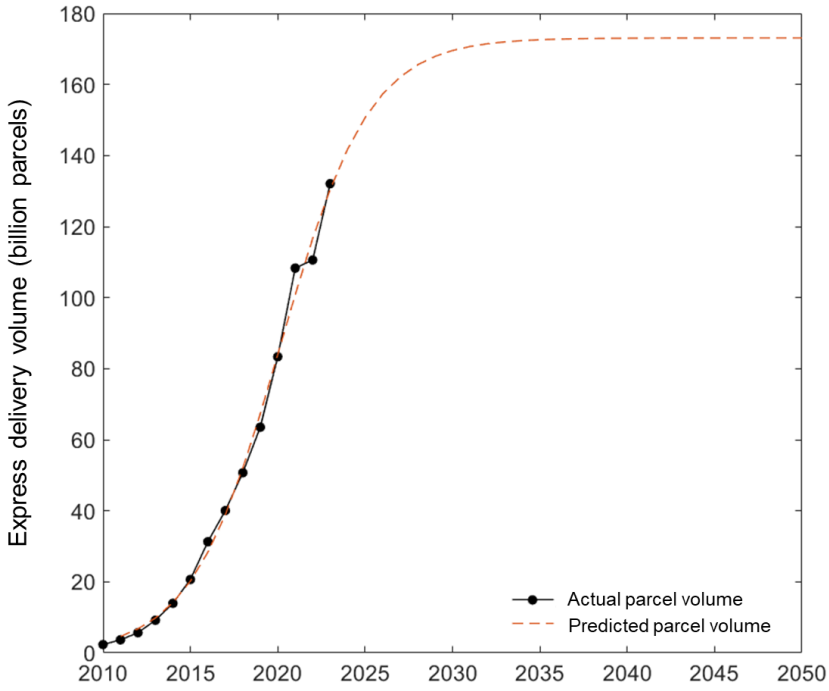

Fig. S10 | Projection of express delivery volume in China through 2050. Historical data (2010-2023, n=14 years) fitted with logistic growth model (R^2=0.99, $p<0.001$).

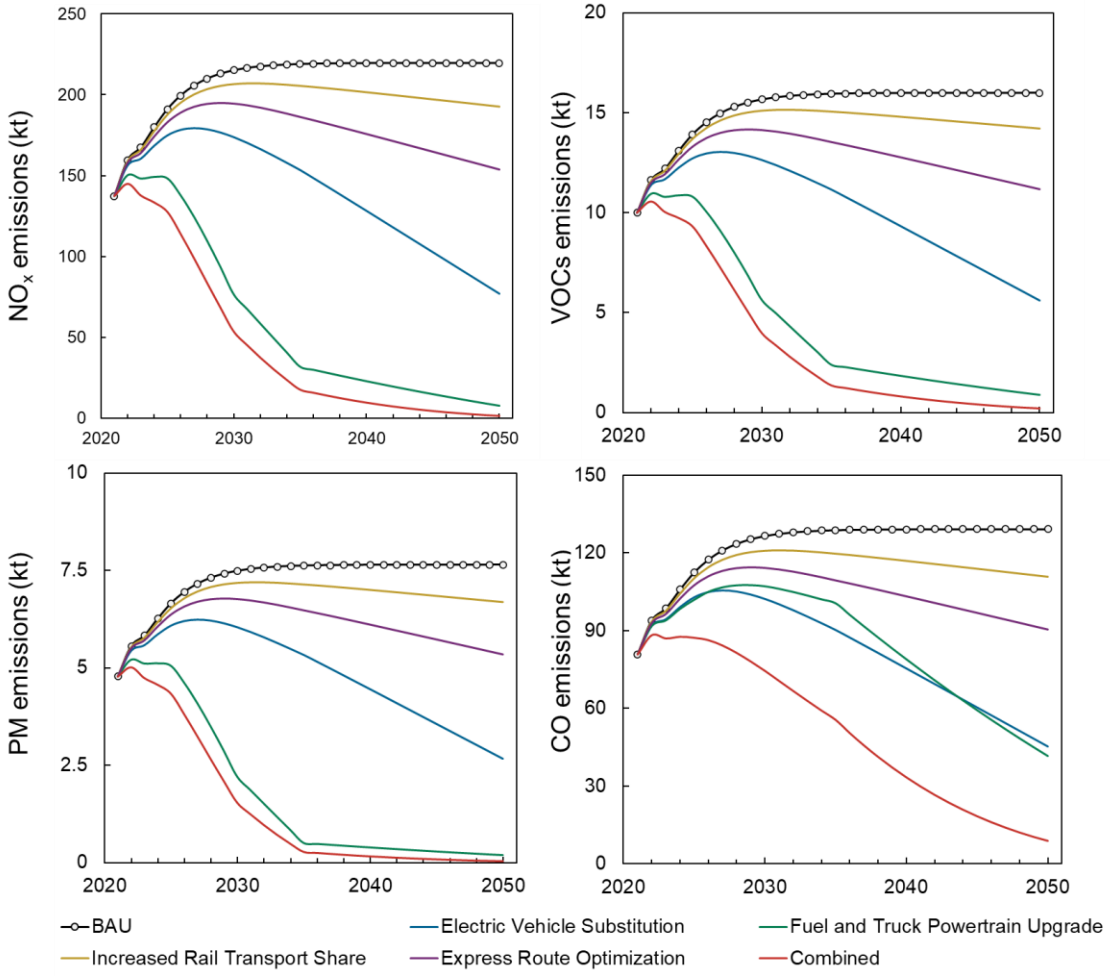

Fig. S11 | Projections of air pollutant emissions from express delivery transportation through 2050.

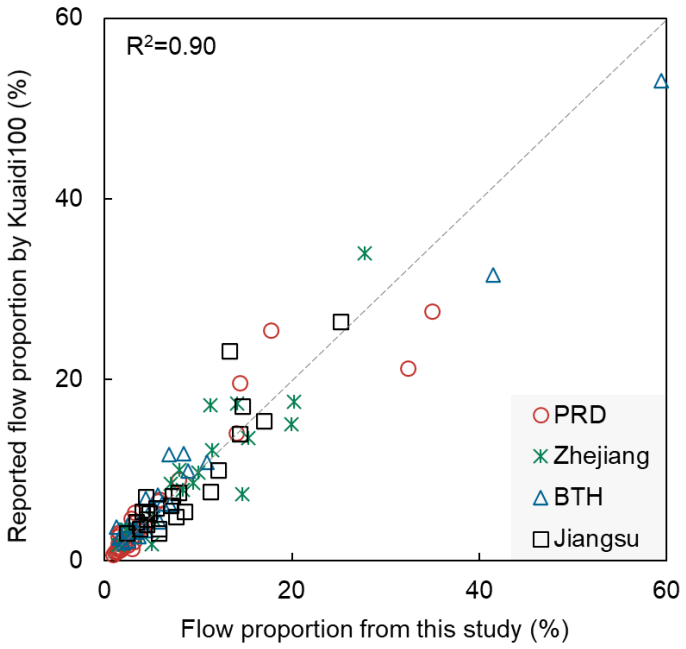

Fig. S12 | Validation of inter-city parcel flow patterns. Scatter plot showing the correlation between parcel flow proportions derived from this study and those reported by Kuaidi100 platform based on their 12.97 million delivery records (R^2=0.90, p<0.001). Each point represents the percentage of parcels flowing from a major city (Beijing, Tianjin, Guangzhou, Shenzhen, Suzhou, Nantong, Jinhua, or Hangzhou) to another city within its region (n=105 city pairs).

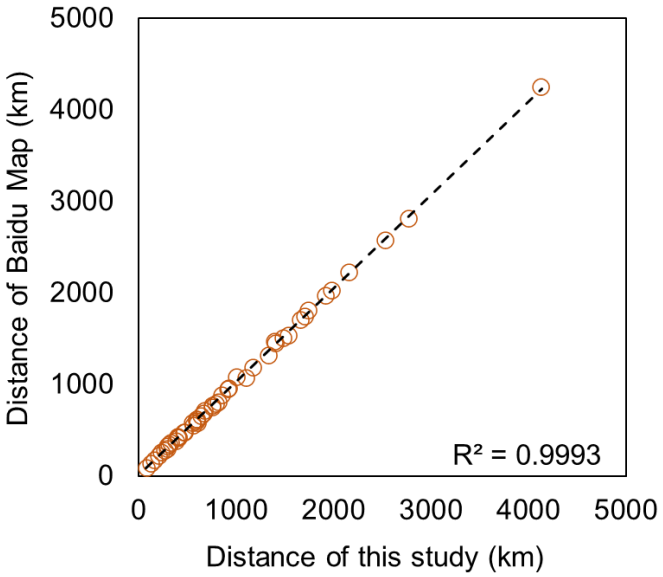

Fig. S13 | Validation of route distance estimation. Comparison between route distances derived from Baidu Maps (a widely-used navigation platform in China) and this study for randomly selected express delivery routes (n=50 routes, R^2=0.999, p<0.001, NMB=2.8%). The high R^2 value reflects the consistent distance calculations on fixed road networks, while the small NMB indicates minor systematic differences in route selection algorithms.

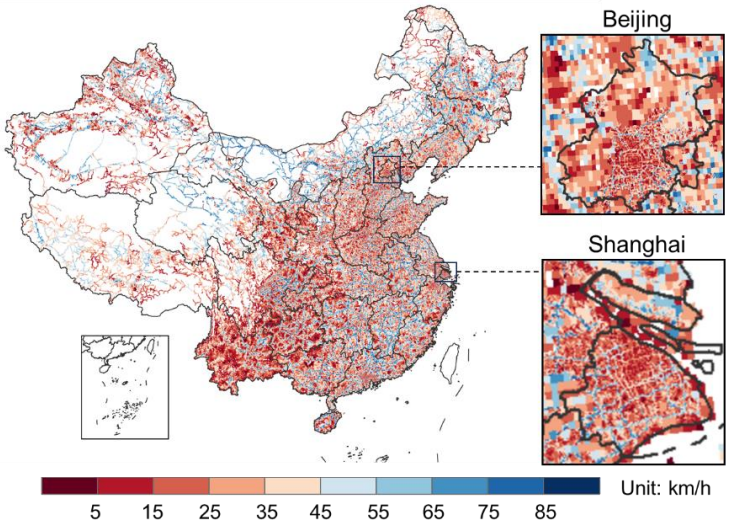

Fig. S14 | Daily average vehicle speed across China (km/h). Map was created using ArcGIS (v10.8, Esri), with administrative boundaries from the Standard Map Service System, Ministry of Natural Resources of China (http://bzdt.ch.mnr.gov.cn/index.html).

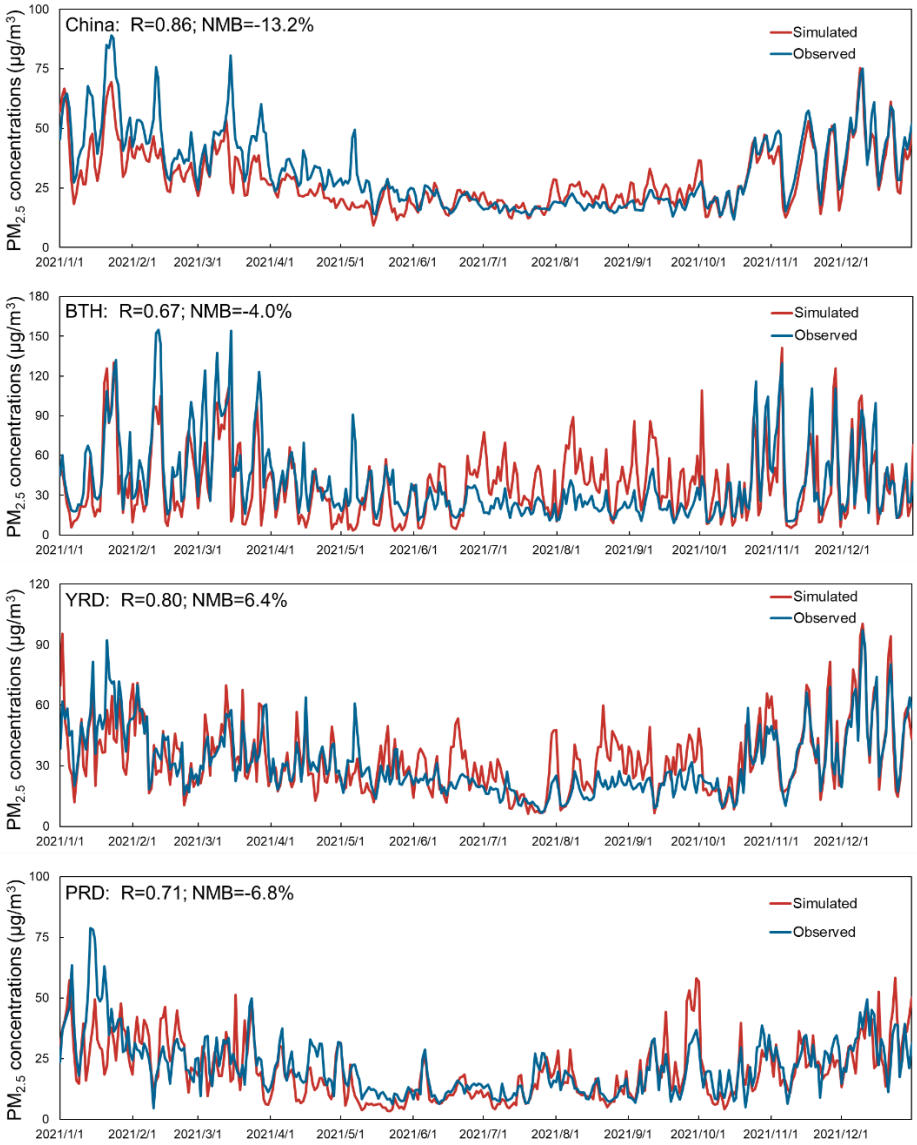

Fig. S15 | Model performance evaluation for $PM_{2.5}$. Comparison between observed and GEOS-Chem simulated daily $PM_{2.5}$ concentrations (μg/m^3) across China (n=365 days, R=0.86, p<0.001, NMB=-13.2%) and in three major urban agglomerations: Beijing-Tianjin-Hebei (BTH: n=365 days, R=0.67, p<0.001, NMB=-4.0%), Yangtze River Delta (YRD: n=365 days, R=0.80, p<0.001, NMB=6.4%), and Pearl River Delta (PRD: n=365 days, R=0.71, p<0.001, NMB=-6.8%).

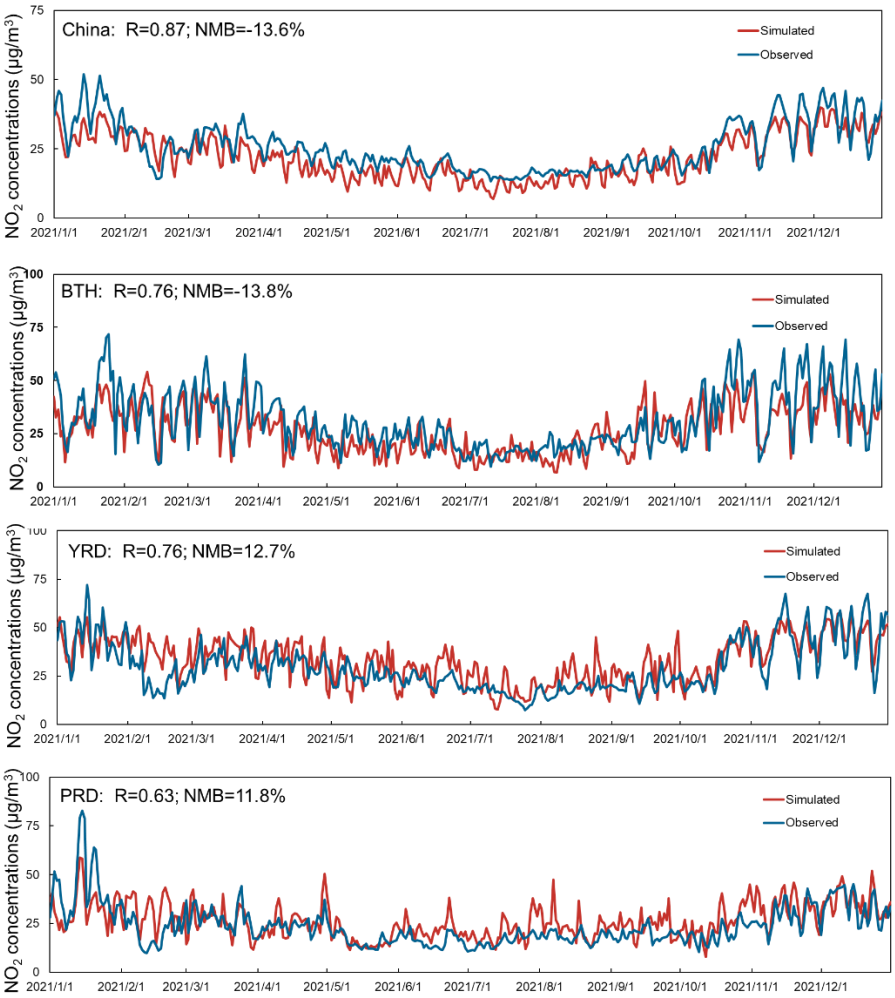

Fig. S16 | Model performance evaluation for NO_2. Comparison between observed and GEOS-Chem simulated daily NO_2 concentrations ($\mu g/m^3$) across China (n=365 days, R=0.87, p<0.001, NMB=-13.6%) and in three major urban agglomerations: Beijing-Tianjin-Hebei (BTH: n=365 days, R=0.76, p<0.001, NMB=-13.8%), Yangtze River Delta (YRD: n=365 days, R=0.76, p<0.001, NMB=12.7%), and Pearl River Delta (PRD: n=365 days, R=0.63, p<0.001, NMB=11.8%).

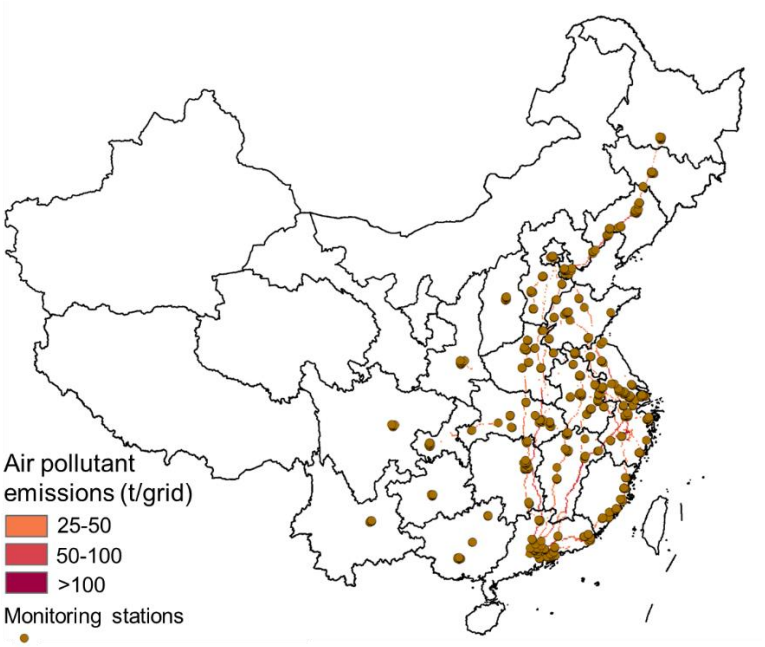

Fig. S17 | Locations of monitoring stations near high express delivery emission areas. Monitoring stations (n=541) located in or within 5 arcmin distance of high-emission grids (defined as grids with express delivery emissions exceeding 25t per 5 arcmin grid). The map was created using ArcGIS (v10.8, Esri), with administrative boundaries from the Standard Map Service System, Ministry of Natural Resources of China (http://bzdt.ch.mnr.gov.cn/index.html).

Table S1 | An example of express delivery waybill tracking information.

Date	Location	Status	Details
2021/12/07 17:xx	Suzhou	Collected	Collected at xx Branch, courier: Name, Tel: 139xxxxxxxx
2021/12/07 17:xx	Suzhou	In Transit	Departed from xx Branch to Suzhou xx Processing Center
2021/12/07 17:xx	Suzhou	Arrived	Arrived at Suzhou xx Processing Center
2021/12/07 23:xx	Suzhou	In Transit	Departed from Suzhou xx Processing Center to Nanjing xx Center
2021/12/08 02:xx	Nanjing	Transfer	Arrived at Nanjing xx Center (Transfer)
2021/12/08 17:xx	Nanjing	In Transit	Departed from Nanjing xx Center to Guiyang xx Center (Transfer)
2021/12/08 18:xx	Guiyang	Transfer	Arrived at Guiyang xx Center (Transfer)
2021/12/09 03:xx	Guiyang	In Transit	Departed from Guiyang xx Processing Center to Zunyi xx Center (Transfer)
2021/12/09 09:xx	Zunyi	Arrived	Arrived at Zunyi xx Center
2021/12/10 07:xx	Zunyi	In Transit	Departed from Zunyi xx Center to Zunyi xx Branch
2021/12/10 07:xx	Zunyi	Processing	Received at Zunyi xx Branch, arranging for delivery
2021/12/10 08:xx	Zunyi	Out for Delivery	Arranged for delivery, courier: Name, Tel: 139xxxxxxxx
2021/12/10 10:xx	Zunyi	Delivered	Signed and received at xx, courier: Name, Tel: 139xxxxxxxx

Note: Personal information (time stamps, detailed locations, name and telephone numbers) has been anonymized (marked as 'xx') to protect privacy.

Table S2 | Top 10 Cities by Express Delivery Volume in China, 2021.

Rank	City	Province	Region	Express Delivery Volume (billion)	Proportion of national express delivery volume (%)	proportion of intra-city and inter-city express delivery	
						Intra-city	Inter-city
1	Jinhua	Zhejiang	YRD	11.6	10.7	4.4	95.2
2	Guangzhou	Guangdong	PRD	10.7	9.9	14.8	83.9
3	Shenzhen	Guangdong	PRD	6.0	5.5	19.7	66.8
4	Shanghai	Shanghai	YRD	3.7	3.5	22.1	73.8
5	Hangzhou	Zhejiang	YRD	3.7	3.4	12.8	74.9
6	Jieyang	Guangdong	PRD	3.5	3.3	4.9	95.1
7	Dongguan	Guangdong	PRD	2.7	2.5	15.9	77.9
8	Suzhou	Jiangsu	YRD	2.5	2.3	19.1	80.0
9	Beijing	Beijing	BTH	2.2	2.0	26.8	72.7
10	Quanzhou	Fujian	—	2.2	2.0	8.4	90.9

Note: Data were compiled from the State Post Bureau of China and municipal statistical data[8].

Table S3 | Air pollutant and GHG emissions from intra-city and inter-city express delivery transportation.

Species	Intra-city (kt)	Inter-city (kt)	Total (kt)
CO	1.63	79.18	80.81
NO_x	2.32	135.06	137.39
VOCs	0.33	9.67	10.00
PM	0.08	4.70	4.78
SO_2	0.04	3.94	3.98
NH_3	0.00	0.46	0.46
atmospheric pollutant equivalents	2.97	163.45	166.41
GHG	355.59	23539.22	23894.81

Table S4 | Comparison of GEOS-Chem and WRF-Chem model results for baseline concentrations and express delivery contributions across different region types in the simulation domain (averaged for January, April, July, and October 2021).

	Pollutant	Region type	GEOS-Chem	WRF-Chem
Baseline ($\mu g/m^3$)	$PM_{2.5}$	Full domain	29	25
	NO_2	Full domain	16	15
Express delivery contribution (ng/m^3)	$PM_{2.5}$	Major transit regions	108	120
		Other regions	66	75
	NO_2	Major transit regions	173	183
		Other regions	150	147

Note: The simulation domain is shown in Fig. S8. Transit regions include Jiangxi, Anhui, Henan, Hubei, and Hunan provinces. Both models consistently show higher express delivery contributions in transit regions compared to other regions, supporting our conclusion about cross-regional environmental inequity.

Table S5 | Base emission factors for different vehicle types under various emission standards (g/km)

	Emission Standard	CO	NO_x	VOCs	PM
Heavy-duty	China II	3.08	7.93	0.82	0.56
	China III	2.79	7.93	0.4	0.27
	China IV	2.2	5.55	0.2	0.15
	China V	2.2	4.72	0.2	0.03
	China VI	2.2	0.94	0.06	0.015
Light-duty	China II	3.22	5.58	1.48	0.29
	China III	1.88	3.77	0.42	0.14
	China IV	1.48	2.64	0.21	0.06
	China V	1.48	2.24	0.21	0.01
	China VI	1.48	0.45	0.06	0.005

Notes: Base emission factors for air pollutants (CO, NO_x, VOCs, and PM) were obtained from the national handbook of vehicle emissions[9, 10]. The actual emission factors used in calculations were further adjusted for speed and environmental factors[9, 11, 12].

Table S6 | Projected demographic composition of China by age groups through 2050 (proportion of total population, %)

Age group	2021	2025	2030	2035	2040	2045	2050
25-29	6.1	5.3	5.0	5.6	6.3	7.4	6.3
30-34	8.6	6.4	5.3	5.0	5.7	6.5	7.6
35-39	7.3	8.7	6.4	5.3	5.0	5.8	6.6
40-44	6.6	6.8	8.5	6.3	5.3	5.0	5.8
45-49	7.7	6.4	6.7	8.4	6.3	5.3	5.0
50-54	8.7	7.8	6.2	6.6	8.3	6.2	5.3
55-59	8.2	8.2	7.5	6.0	6.4	8.1	6.1
60-64	4.7	6.8	7.8	7.2	5.8	6.2	8.0
65-69	5.4	4.7	6.2	7.2	6.7	5.4	5.8
70-74	3.8	4.6	4.2	5.5	6.4	6.0	4.9
75-79	2.3	2.8	3.6	3.3	4.4	5.2	4.9
80+	2.7	2.7	3.1	4.0	4.3	5.2	6.2

SI References

1. Kang, P. et al. Low-carbon pathways for the booming express delivery sector in China. *Nat. Commun.* **12**, 450 (2021).
2. Liang, X. et al. Parcels and mail by high speed rail–A comparative analysis of Germany, France and China. *Journal of Rail Transport Planning & Management* **6**, 77-88 (2016).
3. Chen, H. Study on the general layout of express delivery electric car. Master's thesis, Chang'an University, Xi'an, China (2020).
4. Wang, L. et al. Switching to electric vehicles can lead to significant reductions of $PM_{2.5}$ and NO_2 across China. *One Earth* **4**, 1037-1048 (2021).
5. Buldeo Rai, H., Touami, S. & Dablanc, L. Not all e-commerce emits equally: Systematic quantitative review of online and store purchases' carbon footprint. *Environ. Sci. Technol.* **57**, 708-718 (2022).
6. *Greenhouse Gas Accounting Methods and Reporting Guidelines for Chinese Civil Aviation Enterprises* (National Development and Reform Commission, 2013); https://www.gov.cn/gzdt/att/att/site1/20131104/001e3741a2cc13e13f370a.pdf
7. Ma, S. et al. Exploring emission spatiotemporal pattern and potential reduction capacity in China's aviation sector: Flight trajectory optimization perspective. *Sci. Total Environ.* **951**, 175558 (2024).
8. *Operation of China's postal industry in 2021 (in Chinese)* (State Post Bureau of China, 2022); https://www.gov.cn/xinwen/2022-01/15/content_5668333.htm
9. Wen, Y. et al. Updating On-Road Vehicle Emissions for China: Spatial Patterns, Temporal Trends, and Mitigation Drivers. *Environ. Sci. Technol.* **57**, 14299-14309 (2023).
10. *Technical guidelines on emission inventory development of air pollutants from on-road vehicles (on trial)* (Ministry of Ecology and Environment of China, 2023).
11. Sun, S. et al. Vehicle emissions in a middle-sized city of China: Current status and future trends. *Environ. Int.* **137**, 105514 (2020).
12. Li, Y. et al. A study of high temporal-spatial resolution greenhouse gas emissions inventory for on-road vehicles based on traffic speed-flow model: A case of Beijing. *J. Cleaner Prod.* **277**, 122419 (2020).